

The problem of fluid (gas) flow originating during jet injection in a cylindrical apparatus filled with a porous layer of finite height is solved. Pressure and velocity distributions in the layer are obtained. The influence of the walls of the pipe containing a granular layer on the velocity profile of a one-dimensional filtration layer is investigated.

The question of the nature of the gas or fluid-drop stream distribution in porous media is quite important for the analysis of the operation, simulation, and computation of diverse technological apparatuses in which a stationary granular layer or other porous material is used at the working body. Various heat exchangers [2], metallurgical industry apparatuses [3], catalytic chemical reactors [4, 5], etc., are examples. Moreover, in a number of cases, the filtration of a fluid in a stationary granular embankment can be considered as the simplest model of real fluid phase motion in almost homogeneous fluidized beds.

A large quantity of experimental and industrial data about the organization of filtration streams under quite different conditions and apparatuses has been accumulated up to this time. However, theoretical models of many important classes of flows, including jet flows, which would permit generalization of existing data from a single viewpoint are substantially lacking. A comparatively simple linear problem about jet propagation in a bounded porous layer is investigated below, whose solution affords the possibility of making a number of deductions which are useful in purely practical respects.

Let us investigate the motion in a porous layer of height H which is in a cylindrical apparatus of radius R (see Fig. 1). A fluid jet is delivered through an orifice of radius r_0 in the $z=0$ plane of the layer base which is coaxial with the walls of the apparatus; the total mass flow rate Q is considered given, and the mean fluid velocity in the orifice section is $U = Q/(\pi r_0^2)$. It is required to find the fluid velocity and pressure fields in the domain $0 \leq r < R$, $0 \leq z \leq H$.

For definiteness, let us consider the rate of fluid filtration u associated with the mean velocity in the pore space $u^{(i)}$ by the relationship $u = \varepsilon u^{(i)}$. We consider the layer porosity ε homogeneous (it is easy to examine the influence of random fluctuations in ε on the flow directly by using the method developed in [6]). Then the Darcy equations are

$$-\nabla p + d_0 g - \alpha u = 0, \quad \text{div } u = 0. \quad (1)$$

The flow drag αu , exerted by a porous body per unit layer volume, is taken linear in the velocity u , which is strictly valid just for the inertialess filtration mode characterized by small values of the Reynolds number computed with respect to the microstructure scale of the porous material. This force is nonlinear in the inertial mode which is realized quite often for coarsely dispersed granular layers; in that case the quantity αu should be considered as some approximation to the true drag which is valid in a definite range of variation in u .

For the determination of (1) we impose conditions of nonpenetration of the apparatus walls (the normal filtration velocity component vanishes at the walls), symmetry relative to the $r=0$ axis, constancy of the pressure at the upper layer boundary $z=H$, and the condition of jet fluid inflow at the lower boundary (the normal velocity component goes over into a given function U for $r < r_0$ and vanishes for $r_0 \leq r < R$).

Introducing the excess pressure function

Institute of the Problems of Mechanics, Academy of Sciences of the USSR, Moscow. Moscow Institute of Chemical Machine Construction. Translated from *Inzhenerno-Fizicheskii Zhurnal*, Vol. 28, No. 6, pp. 968-976, June, 1975. Original article submitted April 1, 1974.

©1976 Plenum Publishing Corporation, 227 West 17th Street, New York, N.Y. 10011. No part of this publication may be reproduced, stored in a retrieval system, or transmitted, in any form or by any means, electronic, mechanical, photocopying, microfilming, recording or otherwise, without written permission of the publisher. A copy of this article is available from the publisher for \$15.00.

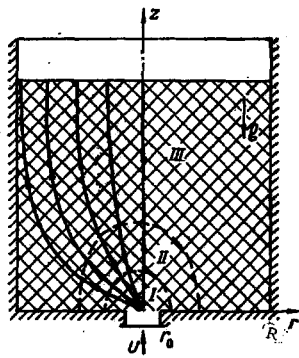


Fig. 1

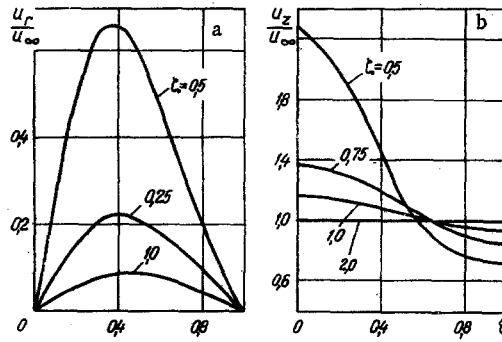


Fig. 2

Fig. 1. Diagram for formulating the problem of jet flow in a porous layer of finite height.

Fig. 2. Characteristic transverse (a) and longitudinal (b) velocity component profiles in a layer of great height.

$$\varphi = p - d_0 g(z - H) \tag{2}$$

and measuring the pressure from its value at $z = H$, we obtain the following problem from (1):

$$\begin{aligned} \Delta\varphi = 0, \quad u = -\alpha^{-1}\nabla\varphi, \\ \varphi < \infty, \quad \partial\varphi/\partial r = 0 \quad (r = 0); \quad \partial\varphi/\partial r = 0 \quad (r = R), \\ \varphi = 0 \quad (z = H); \quad \frac{\partial\varphi}{\partial z} = -F(r) = \begin{cases} -\alpha U, & 0 \leq r < r_0, \\ 0, & r_0 \leq r < R, \end{cases} \quad (z = 0). \end{aligned} \tag{3}$$

Solving the problem (3) by separation of variables, we have the following for an elementary solution satisfying the condition at $r = 0$:

$$C(e^{-\lambda z} + \beta e^{\lambda z}) J_0(\lambda r), \tag{4}$$

where $J_n(x)$ is a Bessel function. Determining the parameter λ and the constant β from conditions (3) for $r = R$ and $z = H$, we obtain the solution in the form of the following superposition of elementary solutions (4):

$$\varphi = \gamma(H - z) + \sum_m C_m (e^{-\lambda_m z} - e^{-\lambda_m(2H-z)}) J_0(\lambda_m r), \quad \lambda_m = \frac{\eta_m}{R}, \tag{5}$$

where γ and C_m are constant coefficients, and η_m are the roots of the equation $J_1(\eta) = 0$.

Using (5), we write the conditions for $z = 0$ in (3) as

$$\gamma + \sum_m \lambda_m (1 + e^{-2\lambda_m H}) C_m J_0(\lambda_m r) = F(r), \tag{6}$$

which can be considered as Dini-Bessel's condition in the function $F(r)$ defined in (3). Using the known definition of the coefficients of this series, we obtain the representation

$$\begin{aligned} \gamma &= \frac{2}{R^2} \int_0^R F(r) r dr = \alpha U \left(\frac{r_0}{R} \right)^2 = \frac{\alpha Q}{\pi R^2}, \\ \lambda_m (1 + e^{-2\lambda_m H}) C_m &= \frac{2}{R^2 J_0^2(\eta_m)} \int_0^R F(r) J_0(\lambda_m r) dr = \frac{2\alpha U}{\eta_m} \cdot \frac{r_0}{R} \cdot \frac{J_1(\lambda_m r_0)}{J_0^2(\eta_m)} = \frac{2\alpha Q}{\pi \eta_m r_0 R} \cdot \frac{J_1(\lambda_m r_0)}{J_0^2(\eta_m)}. \end{aligned} \tag{7}$$

Introducing the dimensionless parameters and mean velocity in the section u_∞ by means of the equalities

$$\{\xi, \xi_0, \zeta, h\} = R^{-1}\{r, r_0, z, H\}, \quad u_\infty = (\pi R^2)^{-1} Q, \tag{8}$$

we finally obtain from (5) and (7)

$$\varphi = \alpha u_\infty R \left\{ h - \zeta + \frac{2}{\xi_0} \sum_m \frac{e^{-\eta_m \zeta} - e^{-\eta_m(2h-\zeta)}}{1 + e^{-2\eta_m h}} \cdot \frac{J_1(\eta_m \xi_0) J_0(\eta_m \xi)}{\eta_m^2 J_0^2(\eta_m)} \right\}. \tag{9}$$

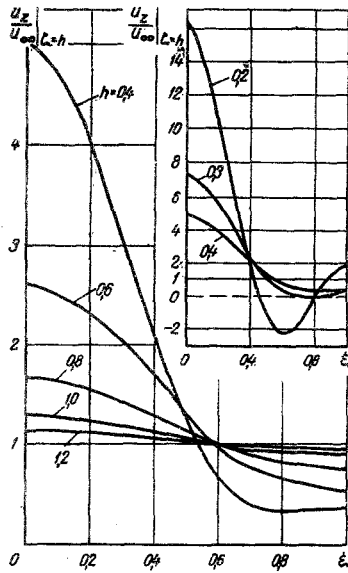


Fig. 3

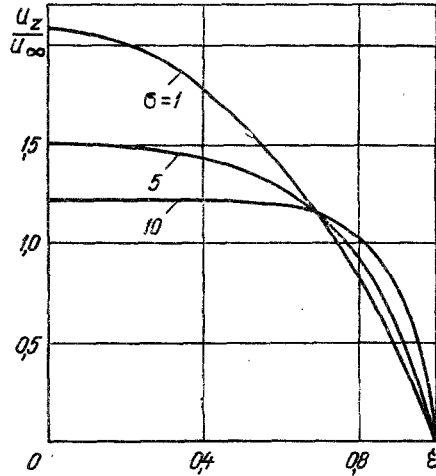


Fig. 4

Fig. 3. Velocity profiles at the upper layer boundary for layers of different heights.

Fig. 4. Dependence of the velocity profile on the parameter σ for $T=1$.

The summation in (9) is performed over all roots of the function $J_1(\eta)$ in increasing order. The velocity components can easily be calculated from (9) in conformity with (3) and the true pressure can be computed by using (2).

In real situations ordinarily $r_0 \ll R$, $r_0 \ll H$. Considering the external flow domain (domain III in Fig. 1) in which the inequalities $\xi_0 \ll \xi$, $\xi_0 \ll \zeta$ are satisfied, but $\xi \ll 1$, $\zeta \ll h$, we obtain approximately from (3) and (9)

$$\varphi = \alpha u_\infty R \left\{ h - \zeta + \sum_m \frac{e^{-\eta_m \zeta} - e^{-\eta_m (2h - \zeta)}}{1 + e^{-2\eta_m h}} \cdot \frac{J_0(\eta_m \xi)}{\eta_m J_0^2(\eta_m)} \right\},$$

$$\frac{u_r}{u_\infty} = \sum_m \frac{e^{-\eta_m \zeta} - e^{-\eta_m (2h - \zeta)}}{1 + e^{-2\eta_m h}} \cdot \frac{J_1(\eta_m \xi)}{J_0^2(\eta_m)}, \quad (10)$$

$$\frac{u_z}{u_\infty} = 1 + \sum_m \frac{e^{-\eta_m \zeta} + e^{-\eta_m (2h - \zeta)}}{1 + e^{-2\eta_m h}} \cdot \frac{J_0(\eta_m \xi)}{J_0^2(\eta_m)}.$$

The expressions (10) are independent of the orifice radius r_0 , which corresponds to the extensively known representation of a real jet far from the site of its injection as a "jet-source" escaping from a point orifice (see [7], for example). Moreover, it can be asserted that the external asymptotic expansions (10) which describe the flow field in domain III are also independent of the orifice shape and its velocity diagram. The latter justifies use of the assumption about the uniform velocity distribution in the injected jet section made in (3).

In high layers, when $h \gg \zeta \gg 1$, the formulas (10) simplify considerably. In this case it is sufficient to take account of just several members in the series (10). Characteristic profiles of the velocity components u_z and u_r , computed from (10) taking into account just the members corresponding to $\eta_1 \approx 3.8$ and $\eta_2 \approx 7.0$, are illustrated in Fig. 2 in the particular case of a high layer $h \rightarrow \infty$. As follows from (10) and from Fig. 2, the velocity on the jet axis $(u_z/u_\infty)_{r=0}$ decreases asymptotically along the length. If the characteristic length of building up the uniform profile l is defined as that value of the coordinate z for which the axial velocity differs by not more than 10% from its asymptotic value u_∞ , then we have

$$l \approx 1.1\zeta. \quad (11)$$

Finally, the velocity distributions u_z on the upper layer boundary are presented in Fig. 3 as a function of its dimensionless height.* The curves of Fig. 3 afford a possibility of selecting the height of a layer of given radial dimension R in such a manner as to assure the required steam equilibration at the exit from the layer.

In the domain directly adjoining the orifice (domain I in Fig. 1), the series (9) is quite inconvenient for practical utilization because of its slow convergence. It is simpler to obtain the internal asymptotic which characterizes the flow in the domain mentioned where $\xi \sim \xi_0$, $\zeta \sim \zeta_0$, but $\xi \ll 1$, $\zeta \ll h$, by repeating the solution (3) under the conditions $R \rightarrow \infty$, $H \rightarrow \infty$. Using a Fourier-Bessel integral instead of Dini-Bessel's condition, we obtain

$$\begin{aligned}\varphi &= \frac{\alpha Q}{\pi r_0} \int_0^\infty e^{-\lambda z} J_1(\lambda r_0) J_0(\lambda r) \frac{d\lambda}{\lambda}, \\ u_z &= \frac{Q}{\pi r_0} \int_0^\infty e^{-\lambda z} J_1(\lambda r_0) J_0(\lambda r) d\lambda, \\ u_r &= \frac{Q}{\pi r_0} \int_0^\infty e^{-\lambda z} J_1(\lambda r_0) J_1(\lambda r) d\lambda\end{aligned}\tag{12}$$

instead of (10) by the previous method.

The integrals in (12) can be expressed as series in hypergeometric functions, and the expression for u_r can be written also in terms of the associated Legendre function of the second kind. Therefore, the flow in the interior domain depends essentially on the size of the orifice, but not on the parameters characterizing the shape of the porous layer itself. The practical values of (12) are not very large; however, they turn out to be useful in analyzing the stresses originating in a friable medium in direct proximity to the jet mouth, as well as in studying the heat and mass transport in the near-lattice zone of some reactors.

In the majority of cases there is an intermediate domain in real apparatuses in which the inequalities $\xi_0 \ll \xi$, $\xi_0 \ll \zeta$ and $\xi \ll 1$, $\zeta \ll h$ (domain II in Fig. 1) are satisfied simultaneously. We obtain the intermediate asymptotic which is valid in this domain from (12) by expanding the function $J_1(\lambda r_0)$ in a power series of the argument and by using just the first member of the series. We consequently have

$$\varphi = \frac{\alpha Q}{2\pi\sqrt{z^2 + r^2}}; \quad u = \sqrt{u_z^2 + u_r^2} = \frac{Q}{2\pi(z^2 + r^2)}.\tag{13}$$

The flow in the intermediate domain is dependent on neither the orifice characteristic nor the external layer parameters. The velocity of this flow is directed along the radius-vector from the jet mouth and depends only on the distance to it. The characteristic streamlines in all three motion domains are also shown in Fig. 1.

Let us emphasize that the fluid velocity at any point of the layer is determined entirely by the position of this point, by the total fluid discharge, and by the system geometry, but is independent of the dynamical parameter α characterizing the drag of the porous material.

The results obtained are also applicable to an approximate analysis of jet flow in a broad layer in the presence of a large number of jets issuing from orifices in a grating if half the mean distance between the centers of adjacent orifices is taken as R. Then the formulas presented above will approximately describe the evolution of the flow produced by an individual jet under conditions of motion constrained by adjacent jets. In particular, the height above the grating, where the flow becomes comparatively homogeneous, will be described by (11), as before.

* Shown in Figs. 2 and 3 are velocity profiles computed approximately with terms corresponding just to η_1 and η_2 taken into account. Such an approximation is degraded with the diminution of ζ or h . Thus, for example, it follows from an examination of the velocity profiles at the exit from the layer in Fig. 3 that the error in the computation becomes significant for $h \leq 0.2-0.3$. For such small h it is certainly necessary to take into account a greater number of terms in the series (10) in the calculations.

Let us note that as follows from an analysis, the gravity field affects just the true pressure p in the layer, but the excess pressure φ and the fluid velocity u are independent of it. This means that the formulas obtained are valid for an arbitrary location of the apparatus in space (for example, for horizontal injection of the jet when g is normal to the z axis, for injection from above, etc.).

As follows from (10), the velocity profile u_z approaches the rectilinear $u_z = u_\infty$ with the increase in ξ . It is interesting to clarify under which conditions this asymptotic profile will actually be almost rectilinear. This problem is of considerable independent interest, since profiles of quite distinct form are observed in real apparatuses [1-5], and any general rule permitting the prediction of the realization of a profile of some kind is unknown.

From the physical viewpoint, the distortion of a rectilinear profile is due to two factors. Firstly, the apparatus walls exert a decelerating effect on the flow which is especially substantial in the near-wall region where the velocity gradients are relatively large. Secondly, for grainy layers the local porosity in direct proximity to the wall is ordinarily greater than in the core of the layer. This latter results in a lowering of the drag in this layer and in the possibility of the fluid "passing through." If the first factor predominates, the maximum filtration velocity is reached at the center of the pipe, but this velocity is almost zero at the wall [8]. If the second factor is more substantial, the limit filtration velocity does not vanish upon approaching the wall, and in a number of cases the maximum velocity is located precisely near the wall. Profiles of both kinds are observed in experiments [1-5].

Limiting ourselves to an analysis of one-dimensional stationary flow in a pipe filled with a porous material, let us take account of the presence of a domain of elevated porosity at the wall by using a two-layer model first introduced in [9]. Within the framework of the model, the material is assumed homogeneous everywhere except in a thin "free," near-wall layer in which the porosity is one. This model had successfully been used earlier in investigating the flow of suspensions in capillaries [8, 10].

The free-layer thickness Δ is proportional to the scale of the material microstructure. Using the grain radius a as such a scale for the grainy layer, we write

$$\Delta = ka. \quad (14)$$

According to the Oliver test data from [10], the coefficient k in (14) is approximately 0.7.

Let us write the equations of motion in the stream core and in the free layer:

$$\begin{aligned} \frac{\mu}{r} \cdot \frac{d}{dr} \left(r \frac{du_z}{dr} \right) - \alpha u_z &= -P; \quad 0 \leq r < R - \Delta, \\ \frac{\mu_0}{r} \cdot \frac{d}{dr} \left(r \frac{du_z}{dr} \right) &= -P; \quad R - \Delta \leq r < R, \end{aligned} \quad (15)$$

where μ is the "apparent" viscosity of the fluid being filtered, which differs from its physical viscosity μ_0 and P is the longitudinal excess pressure gradient. The first equation in (15) is a particular case of the modified Darcy equations obtained rigorously in [11], where an estimate of the quantity μ has also been given for moderately concentrated systems ($\varepsilon > 0.7-0.8$). For closely packed grainy layers the exact value of μ is not known but it can be considered that $\mu \sim \mu_0$.

The usual conditions of boundedness and symmetry relative to the $r=0$ axis and the condition that u_z vanish for $r=R$ are imposed on the solution of (15). The condition on the interface $r=R-\Delta$ of the two flow domains is obtained from the following reasoning. Firstly, the fluid velocity should be continuous during passage through this boundary at points in the gaps between particles and should vanish at points on the particles. It hence follows that the filtration velocity u_z which agrees with the true fluid velocity in the free layer should be continuous on the boundary mentioned. Secondly, (15) can be considered as a single equation defined in the whole domain $0 \leq r < R$, but having discontinuous coefficients. Using standard methods of analyzing such equations at surfaces of discontinuity, the continuity conditions for the tangential stress on the boundary $r=R-\Delta$ can easily be found from (15). Thus

$$\begin{aligned} u_z < \infty; \quad \partial u_z / \partial r = 0 \quad (r = 0); \quad u_z = 0 \quad (r = R), \\ u_z |_{R-\Delta-0} = u_z |_{R-\Delta+0}, \quad \mu \frac{du_z}{dr} |_{R-\Delta-0} = \mu_0 \frac{du_z}{dr} |_{R-\Delta+0}. \end{aligned} \quad (16)$$

Omitting simple, but tedious, computations, let us write the solution of the problem (15), (16) as

$$u_z = \frac{P}{\alpha} \left[1 - T \frac{I_0(\sigma\xi)}{I_0(\sigma)} \right]; \quad 0 \leq \xi < 1 - \delta;$$

$$u_z = \left(\frac{PR^2}{2\mu_0} - c \right) (1 - \xi) - \frac{1}{2} \left(\frac{PR^2}{2\mu_0} + c \right) (1 - \xi)^2; \quad 1 - \delta \leq \xi < 1, \quad (17)$$

where the constants T and c are expressed as follows:

$$T = I_0(\sigma) [I_0(\sigma) + \kappa\sigma\delta I_1(\sigma)]^{-1} [1 - \kappa(\sigma\delta)^2],$$

$$c = \frac{PR^2}{2\mu_0} - \frac{P}{\alpha\delta} (1 + T), \quad (18)$$

where $I_n(x)$ is the Bessel function of imaginary argument and the following dimensionless quantities have been introduced:

$$\kappa = \frac{\mu}{\mu_0}; \quad \delta = \frac{\Delta}{R}; \quad \sigma = \left(\frac{\alpha}{\mu} \right)^{1/2} R. \quad (19)$$

Only the principal members of the expansion in the small parameter δ have been taken into account in (17) and (18); it is impossible to neglect the powers of the quantity $\sigma\delta$ in the general case since ordinarily $\sigma \gg 1$ and possibly $\sigma\delta \sim 1$.

It is convenient to express the quantity P in terms of the velocity u_∞ from (8). Neglecting the fluid flow in the thin near-wall layer, we obtain the expression

$$P = \alpha u_\infty \left[1 - \frac{2T}{\sigma} \cdot \frac{I_1(\sigma)}{I_0(\sigma)} \right] \quad (20)$$

from the condition of equality of the total stream to a given quantity Q.

Let us investigate the velocity profile in the stream core in greater detail. From (17) and (20) we have

$$\frac{u_z}{u_\infty} = \left[1 - \frac{2T}{\sigma} \cdot \frac{I_1(\sigma)}{I_0(\sigma)} \right]^{-1} \left[1 - T \frac{I_0(\sigma\xi)}{I_0(\sigma)} \right], \quad (21)$$

i.e., the profile depends on two parameters, T from (18) and σ from (19).

Let $\sigma\delta \ll 1$ (either the free layer is quite thin or the drag in the grainy layer is low). Then $T \approx 1$, the velocity at the wall equals zero in conformity with (21), and we actually arrive at a solution of the same kind as had been obtained earlier in [8]. The profile u_z depends on σ by changing from the parabolic at $\sigma \approx 0$ to the rectangular at $\sigma \rightarrow \infty$ (see Fig. 4). Therefore, the presence of a porous material in the pipe results in improvement in the velocity profile in the whole flow with the exception of the near-wall region where its steepness is increased.

Now, let $\sigma\delta \gg 1$. In this case, T from (18) is less than one and the velocity limit (21) differs from zero on approaching the wall. Indeed, taking into account that $I_n(\sigma) \gg 1$ for $\sigma \gg 1$, we have from (21)

$$\frac{u_z|_{\xi=1-\delta}}{u_z|_{\xi=0}} = 1 - T. \quad (22)$$

Two situations are possible. If $T > 0$ (the product $\sigma\delta$ is not too large), the velocity has a maximum at the pipe center, as before, but increases monotonically in the free layer from zero at the wall to the limit value determined in (22) at the boundary $r = R - \Delta$. If $T < 0$, then this limit value is greater than the velocity at the pipe axis, and the velocity has a maximum in the free layer. The critical value of the quantity $\sigma\delta$ at which T vanishes is

$$(\sigma\delta)_* = \kappa^{-1} = \mu_0/\mu. \quad (23)$$

Let us note that the relationship (23) can turn out to be useful in estimating μ from experiments.

As follows from an analysis, the filtration velocity profile is actually almost rectilinear in the whole apparatus cross section, for $\sigma \gg 1$, except in a very narrow near-wall zone whose characteristic thickness decreases with the growth in σ .

It has been assumed implicitly above that the continuity of the material is conserved during jet propagation. This assumption is false for high discharges Q and small orifice dimensions r_0 for grainy layers when the formation of practically particle-free caverns or channels is possible near the orifice [12]. However, determination of the conditions for local spoilage of the continuity of the grainy layer and the beginning of channel formation therein is beyond the scope of this paper.

NOTATION

a , radius of grainy layer particle; d_0 , fluid density; F , function in (3); g , acceleration of gravity; H , layer height; h , dimensionless layer height in (8); k , coefficient in (14); l , length of displacement in (11); P , excess pressure gradient; p , pressure; Q , total fluid discharge; R , pipe radius; r , radial coordinate; r_0 , orifice radius; T , parameter in (18); U , mean velocity in the plane of the orifice; u , filtration velocity; u_∞ , asymptotic velocity; z , longitudinal coordinate; α , drag coefficient; Δ , free sublayer thickness; δ , dimensionless thickness in (19); ε , porosity; ξ , dimensionless longitudinal coordinates; η_m , Bessel function roots; κ , ratio between the viscosities in (19); λ_m , parameters in (5); μ , apparent viscosity of the fluid being filtered; μ_0 , physical fluid viscosity; ξ , dimensionless radial coordinate; ξ_0 , dimensionless orifice radius; φ , excess pressure in (2); σ , parameter in (19).

LITERATURE CITED

1. M. É. Aéro and O. M. Todes, Hydraulic and Thermal Operating Principles of Apparatus with a Stationary and Boiling Grainy Layer [in Russian], Khimiya, Leningrad (1968).
2. Z. R. Gorbis, Heat Exchange of Disperse Continuous Streams [in Russian], Énergiya, Moscow — Leningrad (1964).
3. F. F. Kolesanov, Gas Motion through a Layer of Chunky Materials [in Russian], Metallurgizdat (1957).
4. M. É. Aéro and N. N. Umnik, Zh. Prikl. Khim., 27, 602 (1955).
5. P. Co and R. Bibaud, Canad. J. Chem. Eng., 49, 727 (1971).
6. Yu. A. Buevich, Chem. Eng. Sci., 27, 1699 (1972).
7. L. A. Vulis and V. P. Kashkarov, Theory of a Viscous Fluid Jet [in Russian], Nauka, Moscow (1965).
8. Yu. A. Buevich, Izv. Akad. Nauk SSSR, Mekh. Zhidk. Gaza, No. 3, 53 (1968).
9. V. Vand, J. Phys. Colloid Chem., 52, 277 (1948).
10. S. Iwanami and M. Tachibana, Bull. JSME, 12, 224, 231 (1969).
11. Yu. A. Buevich and V. G. Markov, Prikl. Mat. Mekh., 37, 882, 1059 (1973).
12. G. A. Minaev, Author's Abstract of Candidate's Dissertation, Moscow Institute of Chemical Machine Construction (1969).